

The structure and properties of laser seam stepper system (LSS) welded the low alloy high strength steel DOCOL 1200M with martensitic structure

Jacek Górka¹, Andrzej Ozgowicz²

¹ Department of Welding Engineering, Silesian University of Technology, Konarskiego 18A, 44-100 Gliwice, Poland

² Andrzej Ozgowicz, Styvo AS, STRYN, Norway

Abstract: This paper will present the influence of joining process parameters on the structure and properties of overlapped welded joints of 1.8 mm DOCOL 1200M steel. The obtained welded joints were subjected to micro- and macroscopic metallographic examination and hardness measurement. The visual inspections and non-destructive testing made it possible to develop the field of welding parameters to allow obtaining full penetration joints (depending on requirements) or partial penetration joints. For present welding parameters, i.e. feed rate and weld length, which are constant, the actual length of weld is determined by welding frequency. In each case, the microscopic examinations revealed martensitic structure in the weld area, and with the increase in linear welding energy the size of martensite needles became larger, especially in relation to the base material. In HAZ, the martensitic structure is tempered. It has been shown that with appropriately selected parameters the Laser SEAM Stepper method is suitable for welding the DOCOL 1200M steel. With the increase in welding power, the penetration depth increases.

Keywords: DOCOL 1200M steel; Laser SEAM Stepper; welding, martensite

1. Introduction

Steel manufacturers produce newer and newer materials with enhanced properties in response to demand of the automotive industry, among others. This is due to the high requirements regarding the safety of users and the continuous trend towards reducing the weight of produced structures. It allows a considerable reduction in the weight of vehicles, their fuel consumption and harmful gas emissions to the environment. To meet this demand of the automotive industry, the Advanced High Strength Steels (AHSS) were developed. These materials have performed very well in the production of vehicles due to their three very important features: high tensile strength – up to 1700 MPa, high yield point – up to 1450 MPa, and high elongation A80 – up to 30%^[1–9]. It is also important that plastic working and machining of these steels is relatively easy. AHSS are usually used in the automotive industry, because they make it possible to reduce thickness of car body sheets and car body bearing elements, while improving their mechanical properties when compared to conventional steels. The additional advantage of AHSS is their relatively low price due to low amount of alloying additives. Despite the fact that the steels were designed for being joined by bonding processes, some of them still remain a problem for development and optimum parameters of welding method^[10–18]. A great challenge is to join high-strength DOCOL 1200M martensitic steel, primarily intended for car bumpers, side beams and other user-safety elements of motor vehicles. In this respect, the spot welding is still of great importance. The resistance welding technology allows joining metal parts located between the welding electrodes. In the spot welding process, the weld can be made at one or more points at the same time. However, the number of parts to be joined at a single point is limited as up to three

Copyright © 2018 Jacek Górka *et al.*

doi: 10.18063/msacm.v2i1.660

This is an open-access article distributed under the terms of the Creative Commons Attribution Unported License (<http://creativecommons.org/licenses/by-nc/4.0/>), which permits unrestricted use, distribution, and reproduction in any medium, provided the original work is properly cited.

RESEARCH ARTICLE

different elements can be welded only^[19,20]. The resistance spot welding technology is relatively easy to automate and robotise. Because of this, this method for joining metal parts is widely used in the industry. The items that are most often joined in this way are non-alloy and alloy steel sheets for use in household appliances and equipment, electrical and electronic equipment as well as machine components^[19]. The automotive industry is also based on this welding method. The spot welding is applied for joining elements of cars and other vehicles, and in production of car bodies the robotic resistance spot welding cells are used^[20]. An alternative to this method can be the Laser SEAM Stepper (LSS) system developed by IPG Laser GmbH, which combines the advantages of laser-beam welding with the use of attached pressing unit. The LSS system allows welds of up to 40 mm in length to be made, and additionally, at properly present frequency ranging between 3 and 30 Hz, their widths may reach up to 2 mm, which has a significant impact on the strength properties, Figure 1. The standard weld length is approx. 30 mm with uniform spacing between successive passes. The pass rate for this process is about 30 mm/s.

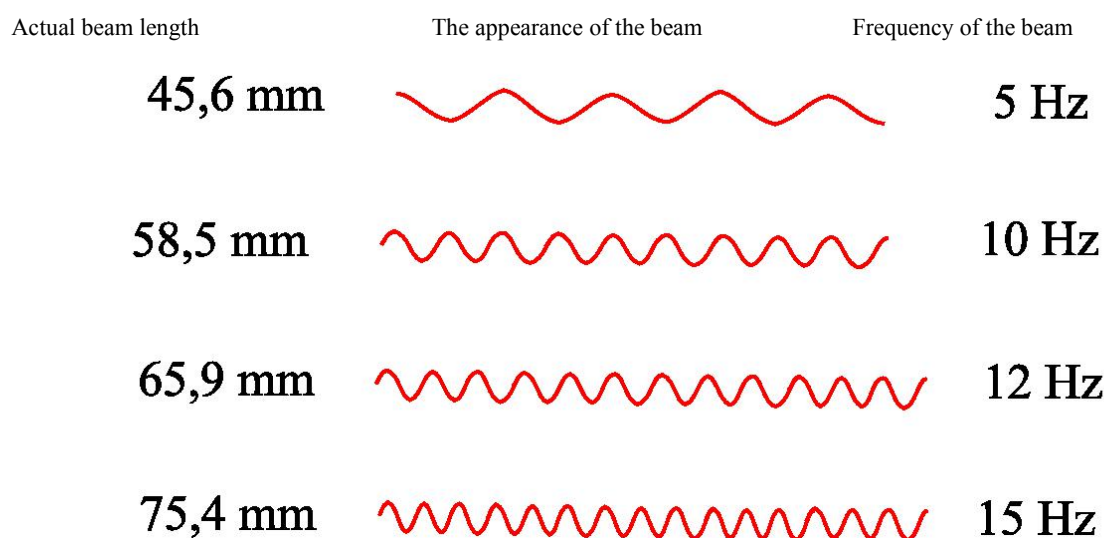


Figure 1. Actual beam length at the frequency used

2. The range of studies

The purpose of the research was to determine the structure and properties of overlap slip joints between the 1.8 mm thick sheets of DOCOL 1200M high-strength low-alloy martensitic steel joined with Laser SEAM Stepper (LSS) technology using variable process parameters: laser beam power, beam feed frequency. The actual chemical composition and properties of DOCOL 1200M steel are presented in Table 1 and its structure – in Figure 2.

Concentration of elements, %											
C	Si	Mn	P	S	Al	Nb	V	Ni	Cr	N	Ce*
0.113	0.22	1.58	0.01	0.002	0.035	0.016	0.01	0.04	0.04	0.006	0.39
Mechanical properties											
Tensile strength Rm, MPa				Yield point Re, MPa				Elongation A ₈₀ , %			
1260				1060				5			
* Ce – carbon equivalent											

Table 1. The chemical composition and mechanical properties of martensitic DOCOL 1200M steel

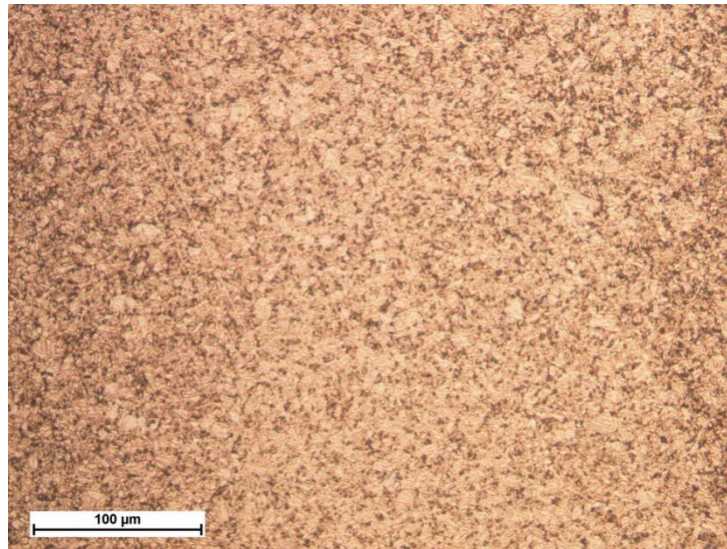


Figure 2. The microstructure of DOCOL 1200M steel

2.1. Joining process

8 test joints were made with variable process parameters using IPG working system, Figure 3. The joining process parameters are summarised in Table 2 and the appearance of joints is shown in Figure 4. In addition, joints for tensile test were made with selected parameters (parameters for joints no. 2, 4, 6, 8).



Figure 3. The view of the Laser SEAM Stepper welding station

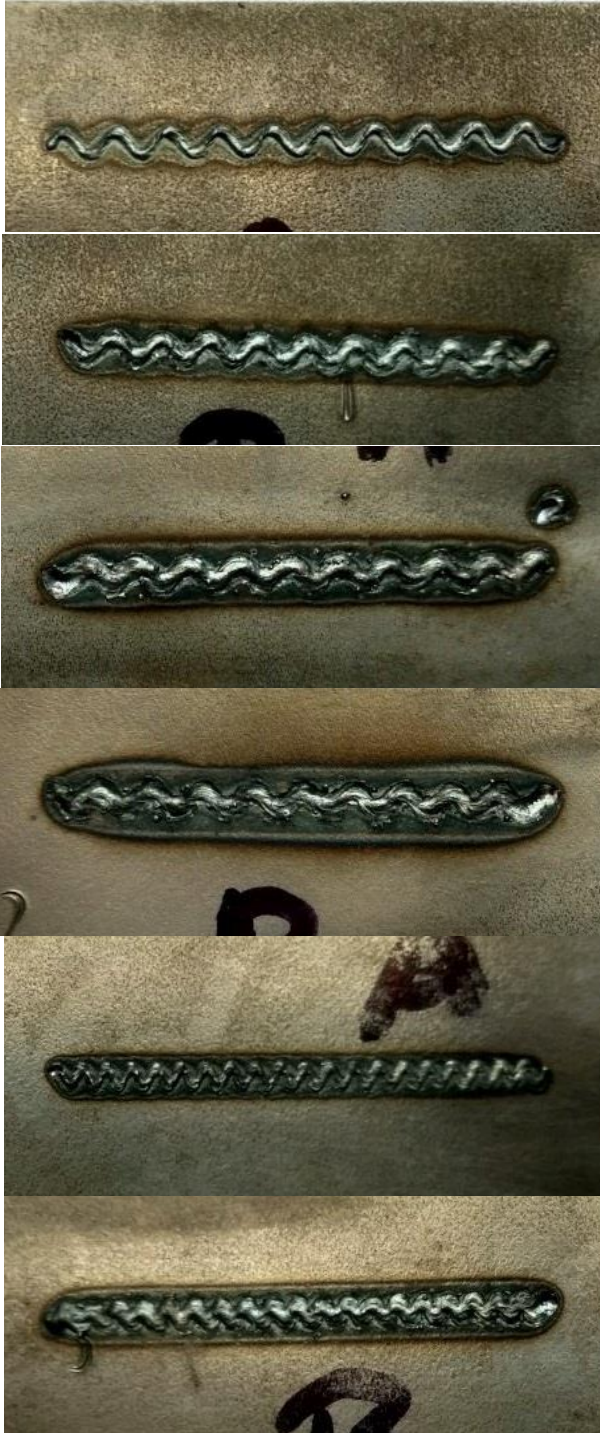
Joint designation	Laser beam power, kW	Feed rate, mm/s	Frequency, Hz	Welding force, N	Weld length, mm	Actual weld length, mm
1	1	20	5	1	40	58
2	1.5					
3	2					
4	2.5					
5	1	20	10	1	40	75
6	1.5					

RESEARCH ARTICLE

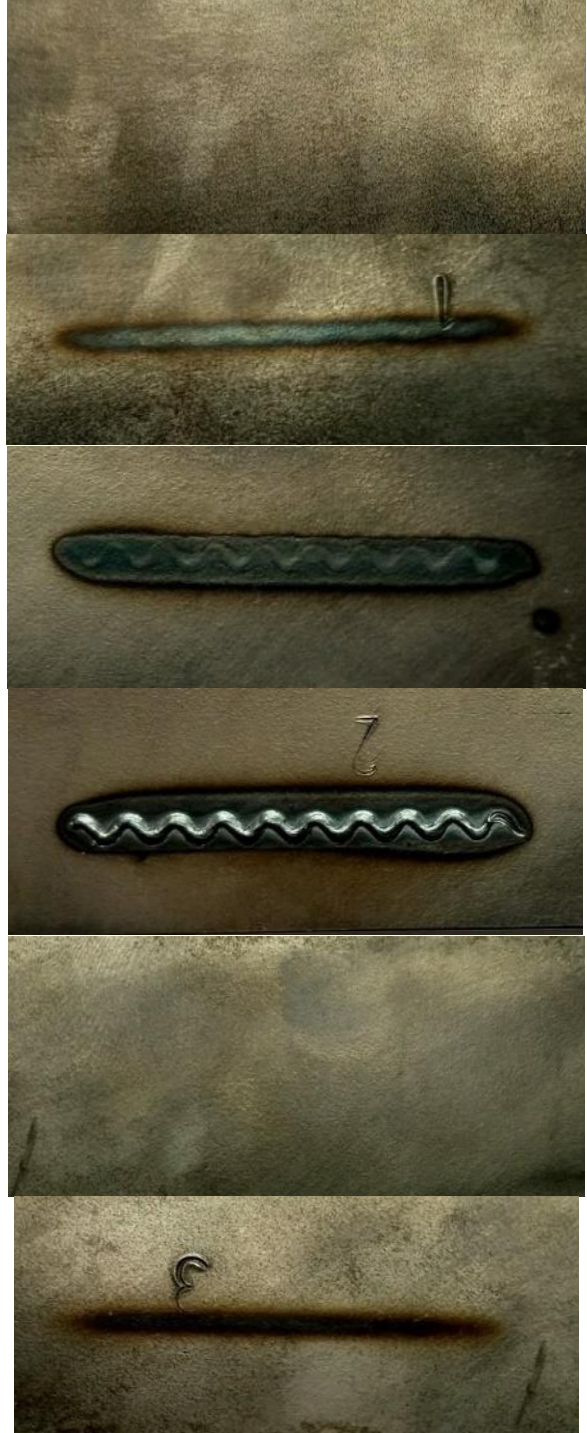
7	2					
8	2.5					

Table 2. Joining process parameters

Weld face



Weld root



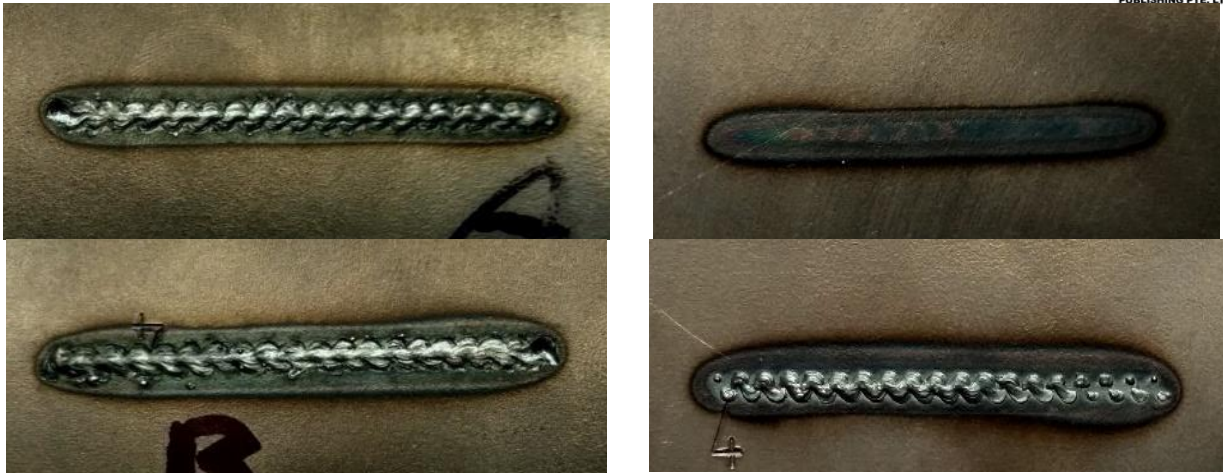


Figure 4. The view from the weld face and root side, order as per Table 2

2.2. Investigations on obtained joints

Following visual inspections, the obtained welded joints were subjected to destructive testing to the following extent:

- macroscopic metallographic examinations using Olympus SZX9 stereoscopic light microscope; the test samples were etched with Adler's reagent;

- microscopic metallographic examinations using NIKON ECLIPSE MA100 light microscope; the test samples were etched with nital;

- hardness measurement using Wilson Wolpert 401MVD Vickers device, under load of 1 kg, taken along a single measuring line in the joint penetration area and HAZ.

- tensile strength tests.

3. Results and Discussion

For joints no. 1 and 3, the used welding parameters did not allow obtaining a satisfactory joint, therefore these joints were excluded from further examinations. The visual inspections of the welded joints revealed no welding defects coming up to the surface, such as cracks and porosity. For joints no. 4 and 8, the visible weld penetration through the sheet can be observed. The macroscopic examinations showed no welding imperfections with regard to shape and geometrical dimensions, Figure 5. In the area of penetration, single gas blowholes appear. These blowholes may occur due to the entrapment of gases dissolved in metal or evaporation of alloying elements or possible impurities at the contact surface between the sheets being joined, Figure 6.



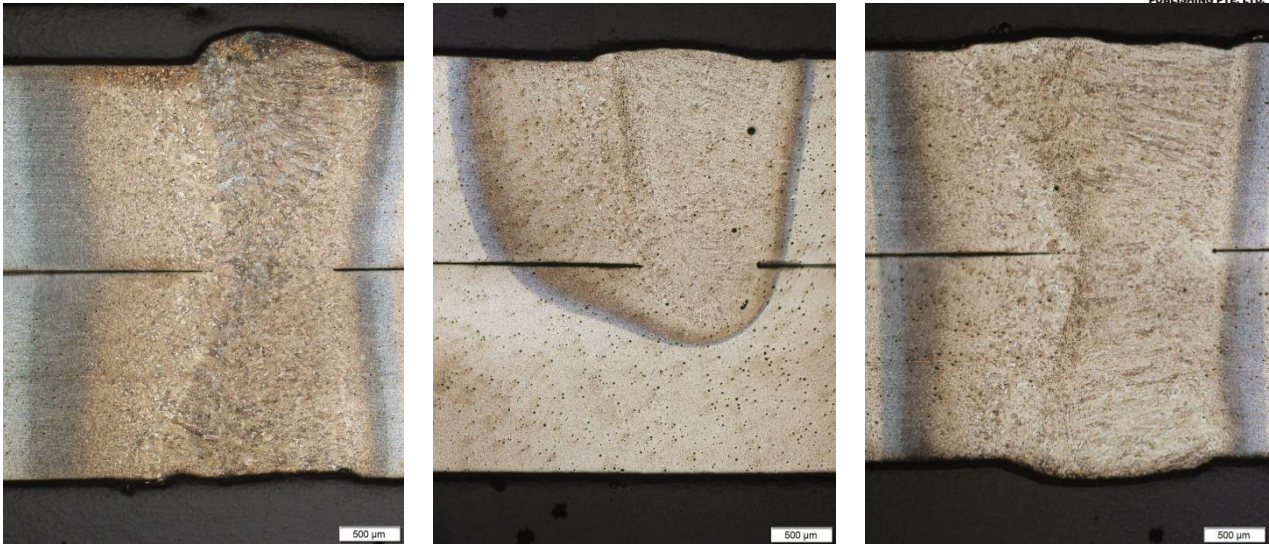


Figure 5. The macrostructure of joints no. 2, 4, 5, 6, 7, 8

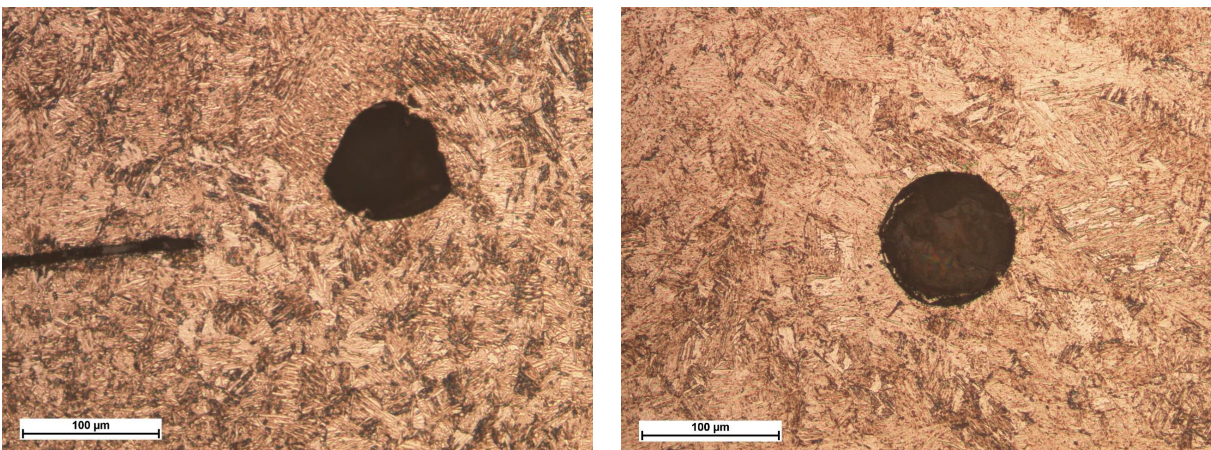


Figure 6. The view of gas blowholes in joints no. 2 and 4

Samples made by the Laser Seam Stepper were subjected to tensile strength test in order to determine whether the type of joining technique and the weld position affect the joint strength. It was noticed that with the increase in the welding laser beam power and frequency, the tensile strength of the joint was increasing. For both longitudinal and transverse joints, the highest strength was shown by joint no. 4, which was welded with the highest power (2.5 kW) and frequency (10 Hz) of the beam, Table 3.

Sample type	Sample number	Force, kN	Place of breaking
	1	26,0	Weld
	2	40,5	
	3	35,5	
	4	49,0	
	5	13,0	Weld
	6	20,5	
	7	25,0	
	8	31,5	HAZ

Table 3. The results of the tensile test

As LSS welding is compared to the resistance spot welding, the basic strength calculations were made. It is assumed that the weld quality classification factors are usually the minimum breaking force, dimensions, acceptable

RESEARCH ARTICLE

internal irregularities and appearance of the weld. Spot-welded joints, made of sheets with a thickness of no more than 3 mm, can be calculated by the method used for determination of the joint's permissible static load (acc. to PN-74/M-69021). For single-cut joints, this load is Eq. (1):

$$F \leq (n \cdot F_n) / x \quad (1)$$

where:

n - number of welds, assumed n = 1,

F_n - the power that destroys the weld,

x - safety factor, assumed x = 2.5.

The longitudinal overlap joints showed no strains occurred during the tensile test. This type of weld position resulted in high results of the permissible static load (even twice as compared to transverse joints), Table 4.

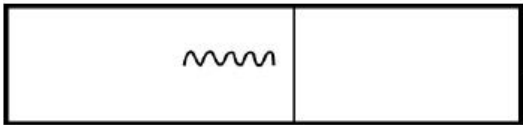
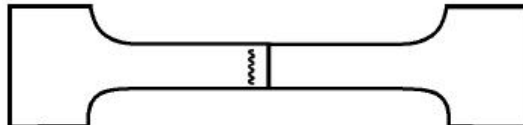
Sample type	Sample number	Permissible permanent load, kN
	1	10,4
	2	16,2
	3	14,2
	4	19,6
	1	5,2
	2	8,2
	3	10,0
	4	12,6

Table 4. Results of permissible constant loads

The microscopic examinations have revealed that the structure of the base material consists of tempered martensite, and in the area of penetrations the acicular martensite exists. On the other hand, the heat affected zone is characterised by structure with visible effects of tempering, Figure 7. A significant increase in grain size in relation to the original size in the base material can be observed. This relationship is visible especially in the area of weld where the grain growth is highest. This is due to the fact that the highest temperatures during the joining process occurred in this area. It should be additionally emphasised that the applied process parameters have also strong impact on grain size in the heat affected zone.



Weld



Fusion line



HAZ



Base material

Figure 7. The microstructure of joint no. 4

The parameters used for welding the joints have a significant impact on hardness of the heat affected zone and the areas of penetration. Hardness of the areas of penetration ranges between 380 and 415 HV 1, depending on the welding process parameters, and is slightly lower than hardness of the base material (440HV1), Figure 8. In HAZ, the tempering process takes place resulting in hardness decreasing to 270 - 320 HV1, Figure 9. The decrease in hardness of these areas may affect the increase in plastic properties of the joints.

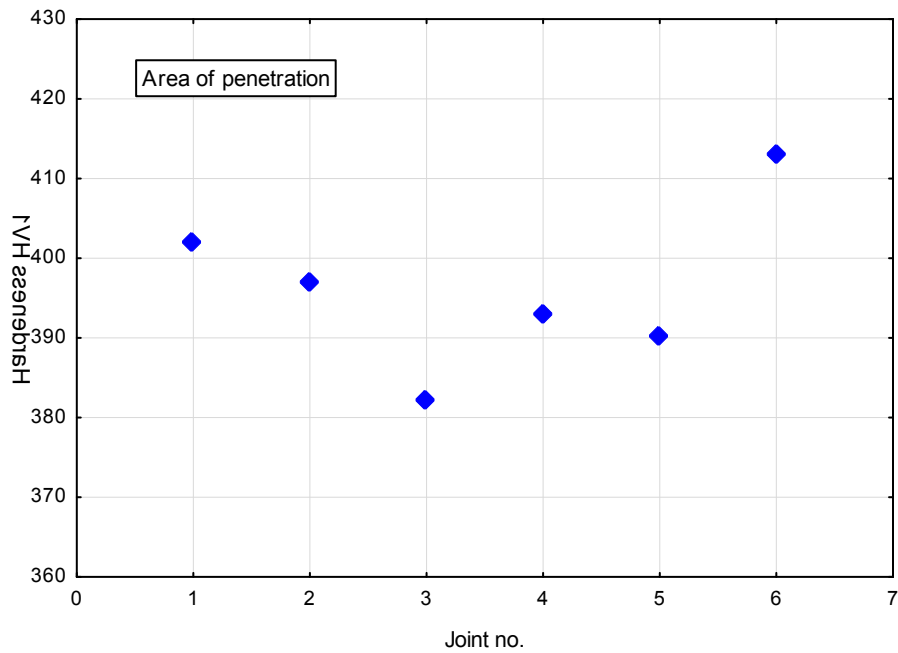


Figure 8. Average hardness of the areas of penetration

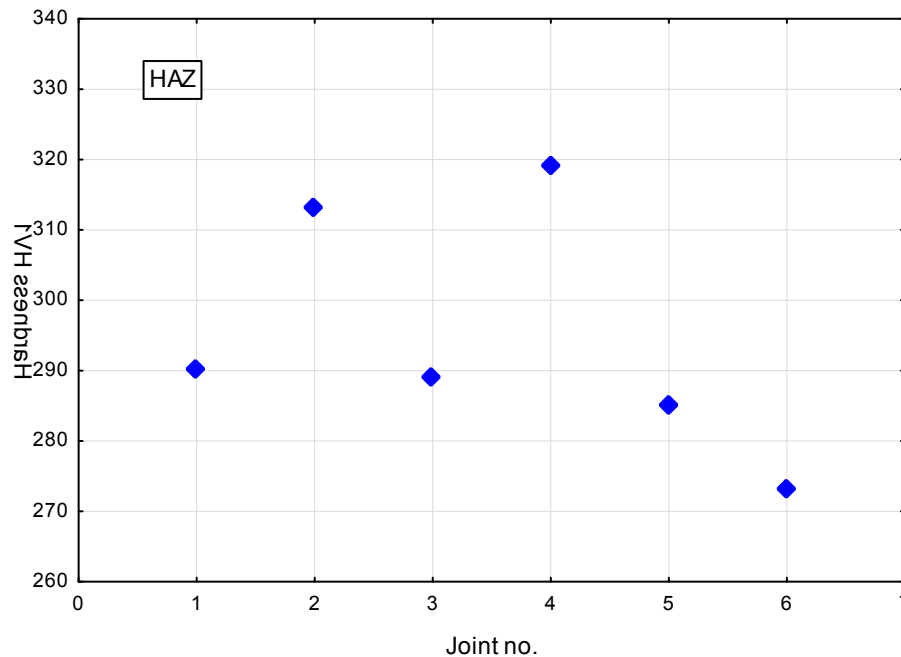


Figure 9. Average hardness of HAZ

4. Conclusions

The examinations carried out on joining of 1.8 mm DOCOL 1200M steels using Laser SEAM Stepper technology have shown that there is a possibility of welding joints that meet the functional requirements. Proper selection of process parameters allows obtaining full penetration (depending on requirements) or partial penetration joints. For tensile strength test, the best results were shown by weld no. 4 (beam power 2.5 kW, frequency 10 Hz), located both along and across the sheets being joined. It was calculated that the longitudinal overlap joint would withstand the static load of 19.6 kN, whereas the transverse overlap joint was characterised by a lower value, 12.6 kN. In the area of penetration, all joints are characterised by acicular martensite structure with variable needle sizes depending on the amount of energy supplied. In HAZ, the native material was tempered resulting in the formation of a softened zone. The size of the weld and the softened zone in the examined joints was increasing with the increase in linear energy of the joining process. To reduce the size of the softened zone, strict process parameters (as short times as possible with high laser beam power) should be used. To limit gas blowholes in the area of penetration, particular attention should be paid to proper cleaning of sheets to remove possible impurities at the contact surfaces between the materials to be joined.

Conflicts of Interest

The author declare no conflict of interest.

References

- Grajcar A, Róžański M. Weldability of high-strength multiphase AHSS steels. *Przegląd Spawalnictwa* No. 3/2014, p. 22–27.
- Nishioka K, Ichikawa K. Progress in thermomechanical control of steel plates and their commercialization. *Science and Technology of Advanced Materials* 2012; 13(2): 1–20.
- Krajewski S, Nowacki J. Microstructure and mechanical properties of Advanced High-Strength Steels (AHSS). *Przegląd Spawalnictwa* No. 7/2011, p. 45–50.
- Stano S. Laser welding of steel sheets differentiated in thickness for designed tailored blanks. *Biuletyn Instytutu Spawalnictwa* No. 2/2005, p. 24–28.
- Chen B, Yu H. Hot ductility behaviour of V-N and V-Nb microalloyed steels. *International Journal of Minerals, Metallurgy and Materials* 2012; 19(6): 525.
- Lee HS, K Park. Evaluation of high strength TMCP steel weld for use in cold regions. *Journal of Constructional Steel Research* 2012; 74: 134–139.
- Górka J. Weldability of thermomechanically treated steels having a high yield point. *Archives of Metallurgy and*

RESEARCH ARTICLE

- Materials 2015; 60(1): 469–475.
8. Lisiecki A. Diode laser welding of high yield steel. Proc. of SPIE Vol. 8703, Laser Technology 2012: Applications of Lasers, 87030S (January 22, 2013).
 9. Adamczyk J, Opiela M. Influence of the thermo-mechanical treatment parameters on the inhomogeneity of the austenite structure and mechanical properties of the Cr-Mo steel with Nb, Ti and B microadditions. Journal of Materials Processing Technology 2004; 157–158: 456–461.
 10. Górka J. Study of structural changes in S700MC steel thermomechanically treated under the influence of simulated welding thermal cycles Indian Journal of Engineering and Materials Sciences 2015; 22: 497–502.
 11. Lisiecki A, Kurc-Lisiecka A. Laser welding of the new grade of advanced high-strength steel Domex 960. Erosion wear resistance of Titanium-Matrix Composite Ti/TiN produced by diode-Laser Gas Nitriding. Materiali in Tehnologije / Materials and Technology 2017; 51(1): 29–34.
 12. Lisiecki A, Kurc-Lisiecka A. Laser welding of the new grade of advanced high-strength steel Domex 960. Materiali in Tehnologije / Materials and Technology 2017; 51(2): 199–204.
 13. Janicki D. Laser cladding of Inconel 625-based composite coatings reinforced by porous chromium carbide particles. Optics & Laser Technology 2017; 94: 6–14.
 14. Janicki D, Muszyfaga-Staszuk M. Direct Diode Laser Cladding of Inconel 625/WC Composite Coatings. Strojniški vestnik - Journal of Mechanical Engineering 2016; 62(6): 363–372.
 15. Grajcar A. Thermodynamic analysis of precipitation processes in Nb-Ti-microalloyed Si-Al TRIP steel. Journal of Thermal Analysis and Calorimetry 2014; 118(2): 1011–1020.
 16. Morawiec M, Róžański M, Grajcar A, *et al.* Effect of dual beam laser welding on microstructure-property relationships of hot-rolled complex phase steel sheets. Archives of Civil and Mechanical Engineering 2017; 17: 145–153.
 17. Opiela M. Thermodynamic analysis of the precipitation of carbonitrides in microalloyed steels. Materiali in Tehnologije 2015; 49(3): 395 – 401.
 18. Opiela M. Elaboration of thermomechanical treatment conditions of Ti-V and Ti-Nb-V microalloyed forging steels. Archives of Metallurgy and Materials 2014; 59(3): 1181–1188.
 19. Grajcar A, Róžański M, Stano S. Effect of heat input on microstructure and hardness distribution of laser welded Si-Al TRIP-type steel. Advances Material Science Engineering 2014; Article ID 658947, pp. 1–8.
 20. Godwin K, Yong O. Microstructure and fatigue performance of butt-welded joints in advanced high-strength steels. Materials Science & Engineering A 2014; 597: 342–348.
 21. Wang W, Li M, He C, *et al.* Experimental study on high strain rate behavior of high strength 600–1000MPa dual phase steels and 1200MPa fully martensitic steels. Materials and Design 2013; 47: 510–521.